10.1071/BT14256_AC

Supplementary Material: *Australian Journal of Botany*, 2015, 63(4), 276–291.

Supplementary Material

Metals and secondary metabolites in saxicolous lichen communities on ultramafic and non-ultramafic rocks of the Western Italian Alps

Sergio E. Favero-Longo[A,D], *Enrica Matteucci*[A], *Mariagrazia Morando*[A], *Franco Rolfo*[B], *Tanner B. Harris*[C] *and Rosanna Piervittori*[A]

[A]Department of Life Sciences and Systems Biology, University of Torino, Viale Mattioli 25, 10125, Torino, Italy.

[B]Department of Earth Sciences, University of Torino, Via Valperga Caluso 35, 10125, Torino, Italy.

[C]College of the Atlantic, 105 Eden Street, Bar Harbor, ME 04609, USA.

[D]Corresponding author. Email: sergio.favero@unito.it

Supplementary Material 1: Location and images of the surveyed plots

Table S1. Location of the surveyed plots

Plot	Area	Lithotype	Datum	Lat	Long (E)
Lhe 1	Mt. Musinè (A)	Lherzolite-Harzburgite	WGS-84	N 45°6.508'	E 7°28.009'
Lhe 2	Mt. Musinè (A)	Lherzolite-Harzburgite	WGS-84	N 45° 6.490'	E 7° 27.877'
Lhe 3	Mt. Musinè (A)	Lherzolite-Harzburgite	WGS-84	N 45°6.639'	E 7°27.569'
Lhe 4	Mt. Musinè (A)	Lherzolite-Harzburgite	WGS-84	N 45°6.627'	E 7°27.574'
Lhe 5	Mt. Musinè (A)	Lherzolite-Harzburgite	WGS-84	N 45° 6.657'	E 7° 27.576'
Dun 1	Mt. Musinè (A)	Dunite	WGS-84	N 45°6.665'	E 7°27.546'
Dun 2	Mt. Musinè (A)	Dunite	WGS-84	N 45° 6.650'	E 7° 27.533'
Ser_A 1	Mt. Musinè (A)	Serpentinite	WGS-84	N 45° 6.712'	E 7° 27.483'
Ser_A 2	Mt. Musinè (A)	Serpentinite	WGS-84	N 45° 6.835'	E 7° 27.289'
Ser_B 1	Monviso (B)	Serpentinite	WGS-84	N 44°41.912'	E 7°5.600'
Ser_B 2	Monviso (B)	Serpentinite	WGS-84	N 44°41.887'	E 7°5.576'
Ser_B 3	Monviso (B)	Serpentinite	WGS-84	N 44°42.120'	E 7°5.497'
MMg 1	Monviso (B)	Mg-Metagabbro	WGS-84	N 44°41.942'	E 7°5.554'
MMg 2	Monviso (B)	Mg-Metagabbro	WGS-84	N 44°41.951'	E 7°5.572'
MMg3	Monviso (B)	Mg-Metagabbro	WGS-84	N 44° 41.909'	E 7° 5.597'

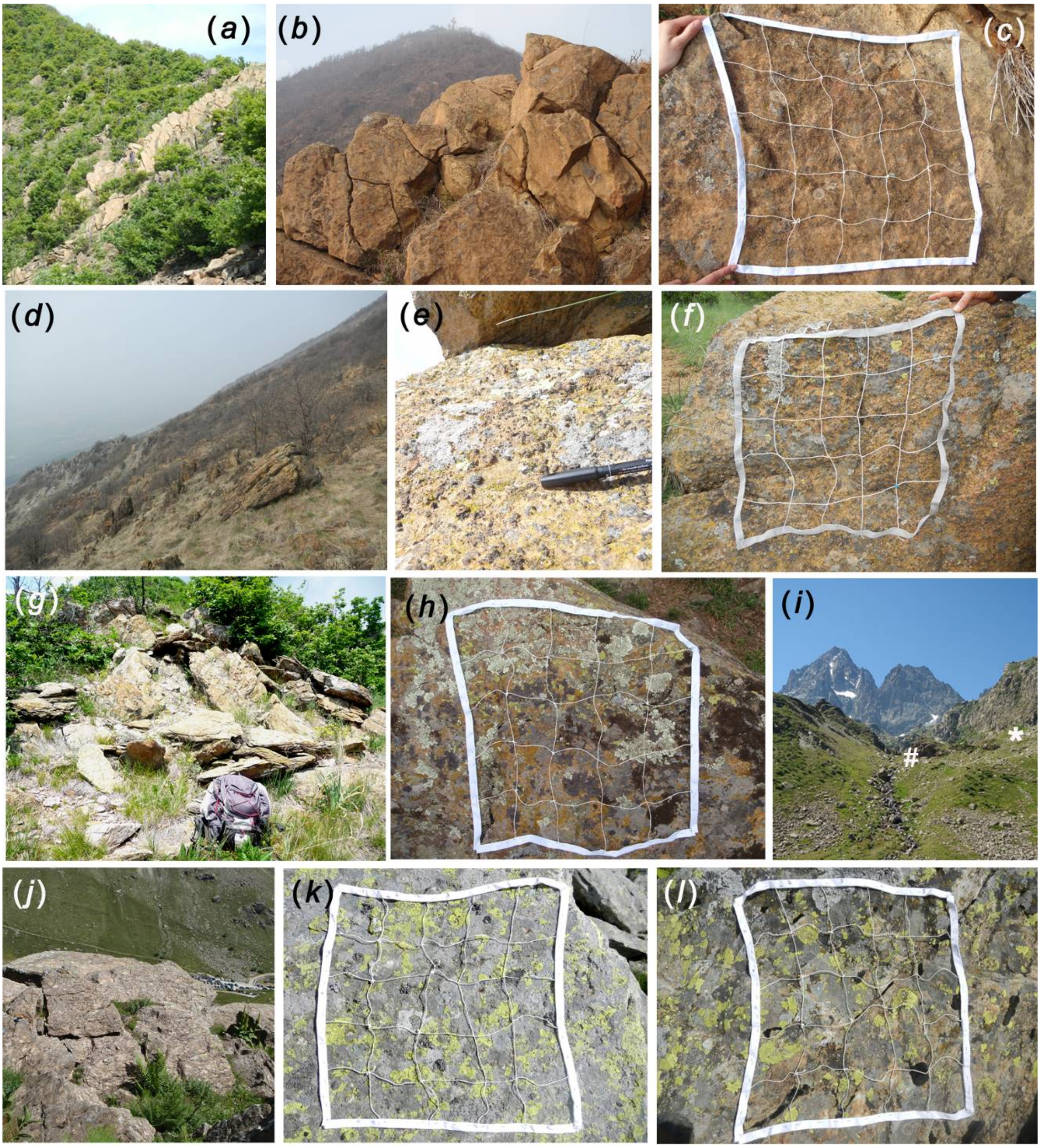

Fig. S1. Images of the Study Areas A (Mt. Musiné: *a*-*h*) and B (Monviso: *i*-*l*). (*a*) Decametre-wide bodies of dunite. (*b*) Outcrop of dunites. (*c*) Representative relevé on dunite (Dun). (*d*) Lherzolite outcrops and blocks. (*e*) Lumpy surface of lherzolite. (*f*) Representative relevé on lherzolite (Lhe). (*g*) Outcrop of serpentinites. (*h*) Representative relevé on serpentinites (Ser_A). (*i*) Study Area B, including outcrops and blocks of serpentinites (#) and blocks of Mg-Al metagabbros (*) from overhanging cliffs. The Monviso summit (3841 m a.s.l.) is visible in the background on the left side. (*j*) Outcrop of serpentinites. (*k*) Representative relevé on Mg-Al metagabbros (MMg). (*l*) Representative relevé on serpentinites (Ser_B).

Supplementary Material 2: Analysis of presence/absence datasets using the SDR-simplex approach: detailed comments on the calculated scores and ternary plots

The SDR analysis indicated that gamma-diversity components were similar if the whole dataset, including relevés on ultramafics and on the mafic MMg, or only the relevés on ultramafics were considered (Table 3 and Fig. S3). Moreover, lower similarity (S) and higher species replacement (R) and richness difference (D) characterized the whole set of relevés on ultramafic rocks (Dun, Lhe, Ser_A, Ser_B), with respect to the dataset of Area B, including Ser_B and MMg.
Slight differences in the SDR values were calculated in Areas A and B when plots on the different lithologies were considered altogether (per area), but remarkable differences characterized the different lithologies. The pairwise similarity among plots was higher on MMg and Ser_B (MMg> Ser_B) than on the lithologies of Area A, which displayed a decreasing trend from Ser_A to Lhe to Dun (i.e. increasing beta diversity, R+D). Strongly higher S values calculated for the separate MMg and Ser_B datasets relative to that calculated for the entirety of Area B suggests differences between the lichen communities on the two lithologies, whereas values calculated on the different lithologies of Area A were relatively closer to that calculated for the whole area, indicating higher homogeneity among lichen communities. Lower R values characterized the lithologies of the alpine Area B relative to those of Area A, where the values increased from Dun to Lhe to Ser_A (i.e. decreasing nestedness, S+D). Similar values of R and D were only observed on Dun and Ser_B, whereas values for R were remarkably higher on the other lithologies. The highest D values were observed on Dun, whereas the lowest values were observed on MMg and Ser_A (i.e. high richness agreement, S+R).

(Table 3 duplicated here to support reading of the detailed comments)

Table 3. Percentage contribution from the SDR Simplex analyses of saxicolous lichen communities in the two study areas

Results are reported for the entire dataset and, separately, for Area A (Mt Musiné) and Area B (Monviso) for the five lithologies (abbreviations in Table 1) and for the overall ultramafics (Dun + Lhe+ Ser_A + SerB)

Dataset	Similarity (S)	Species replacement (R)	Richness difference (D)	Relativised β-diversity (R + D)	Relativised richness agreement (S + R)	Relativised nestedness (S + D)
All areas	28.36	52.91	18.73	71.64	81.27	47.09
Area A	36.75	42.61	20.64	63.25	79.36	57.39
- Dun	41.08	30.85	28.08	58.92	71.92	69.15
- Lhe	42.91	34.89	22.20	57.09	77.80	65.11
- Ser_A	50.60	40.94	8.46	49.40	91.54	59.06
Area B	41.59	42.87	15.54	58.41	84.46	57.13
- Ser_B	56.38	21.72	21.90	43.62	78.10	78.28
- MMg	62.97	24.34	12.69	37.03	87.31	75.66
All ultramafics	31.07	48.16	20.76	68.93	79.24	51.84

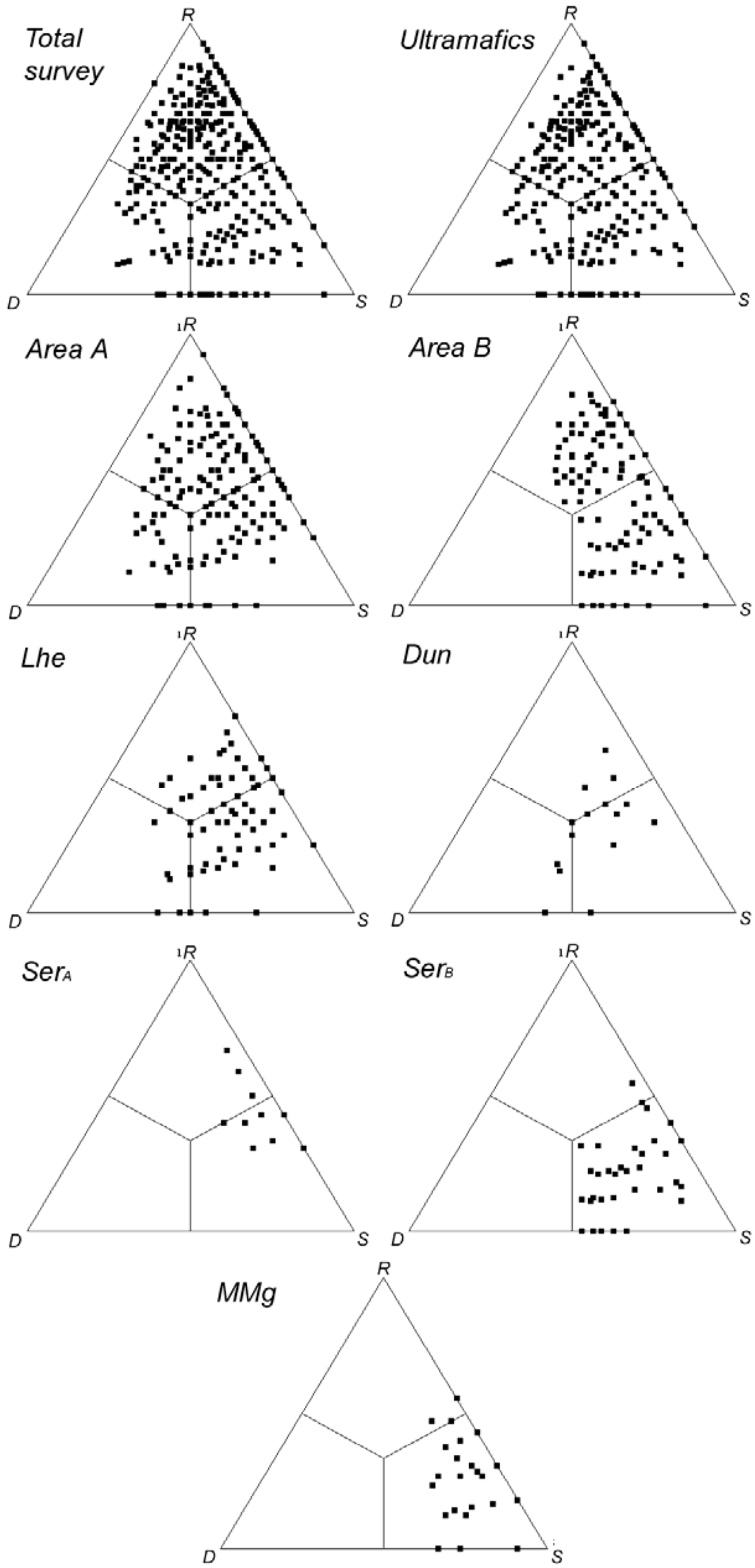

Fig. S3. Ternary plots. S, D, and R refer to relativized similarity, richness difference, and species replacement, respectively.

Supplementary Material 3: PCoA on the matrix of presence/absence of species at the plot level

The PCoA extracted 4 components that accounted for 53.1% of total variance. Plots in Areas A and B are primarily separated along the first axis (24.5% of the total variance). Plots on the different lithologies of Areas A and B are separated along the second (16.6%) and third (6.8%) axes, respectively. Separation between plots of Mt. Musinè (Area A) and Monviso (Area B) is mostly driven by the fact that only a few dominant species (n=9, in bold) are shared by the two areas, whereas the remaining species (n=48) are exclusive to one of the two areas.

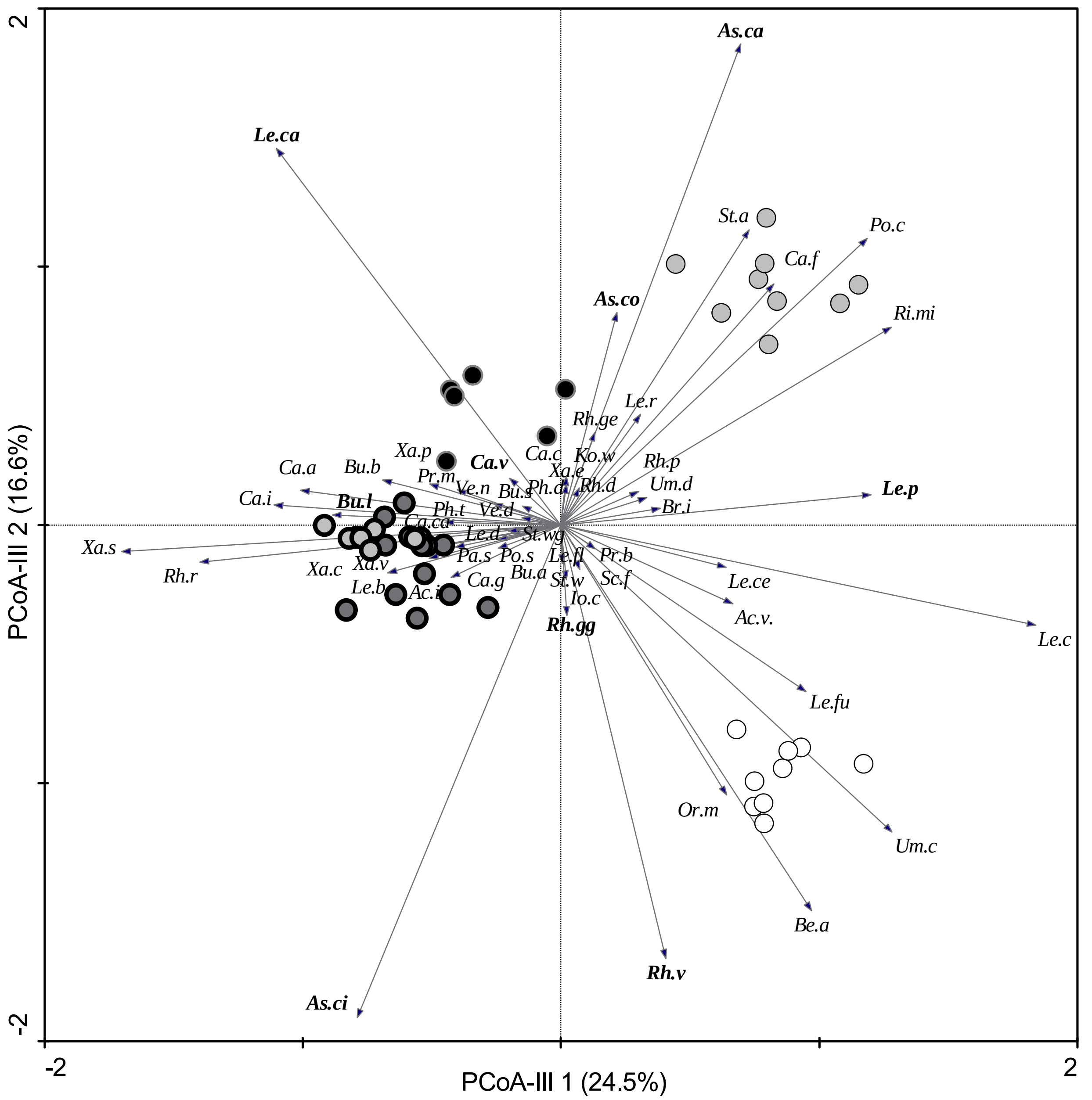

Fig. S2. Ordination of plots on the different lithologies on the basis of species presence/absence. Symbol colours correspond to lithology: dunites (black), lherzolites-harzburgites (dark grey), serpentinites (light grey, with thick border in Area A and thin border in Area B), Mg-metagabbros (white). Species abbreviations are listed in Table S2.

Table S2. Species abbreviations

Species	Abbreviation
Acarospora impressula Th.Fr.	Ac.i
Acarospora veronensis A.Massal.	Ac.v.
Aspicilia caesiocinerea (Malbr.) Arnold	As.ca
Aspicilia cinerea (L.) Körb.	As.ci
Aspicilia contorta ssp. *hoffmanniana* S. Ekman & Fröberg	As.co
Bellemerea alpina (Sommerf.) Clauzade & Cl.Roux	Be.a
Brodoa intestiniformis (Vill.) Goward	Br.i
Buellia aethalea (Ach.) Th.Fr.	Bu.a
Buellia badia (Fr.) A.Massal.	Bu.b
Buellia leptocline (Flot.) A.Massal.	Bu.l
Buellia stellulata (Taylor) Mudd	Bu.s
Caloplaca arenaria (Pers.) Müll.Arg.	Ca.a
Caloplaca cacuminum Poelt	Ca.c
Caloplaca festivella (Nyl.) Kieff.	Ca.f
Caloplaca grimmiae (Nyl.) H.Olivier	Ca.g
Caloplaca irrubescens (Arnold) Zahlbr.	Ca.i
Candelariella vitellina (Hoffm.) Müll.Arg.	Ca.v
Catillaria chalybeia (Borrer) A.Massal.	Or.m
Ionaspis chrysophana (Körb.) Stein	Io.c-Ca.d
Koerberiella wimmeriana (Körb.) Stein	Ko.w
Lecanora bicincta Ramond	Le.b
Lecanora cenisia Ach.	Le.ce
Lecanora dispersa (Pers.) Sommerf.	Le.d
Lecanora flotowiana Spreng.	Le.fl
Lecanora polytropa (Hoffm.) Rabenh. (incl. *L. intricata* (Ach.) Ach.)	Le.p
Lecanora rupicola (L.) Zahlbr.	Le.r
Lecidea confluens (Weber) Ach.	Le.c
Lecidea fuscoatra (L.) Ach.	Le.fu
Lecidella carpathica Körb.	Le.ca
Orphniospora mosigii (Körb.) Hertel & Rambold	Ca.ca
Parmelia saxatilis (L.) Ach.	Pa.s
Physcia dubia (Hoffm.) Lettau	Ph.d
Physcia tribacia (Ach.) Nyl.	Ph.t
Polysporina simplex (Davies) Vězda	Po.s
Porpidia crustulata (Ach.) Hertel & Knoph	Po.c
Protoparmelia badia (Hoffm.) Hafellner	Pr.b
Protoparmeliopsis muralis (Schreb.) M.Choisy	Pr.m
Rhizocarpon distinctum Th.Fr.	Rh.d
Rhizocarpon geminatum Körb.	Rh.ge
Rhizocarpon geographicum (L.) DC.	Rh.gg
Rhizocarpon polycarpum (Hepp) Th.Fr.	Rh.p
Rhizocarpon reductum Th.Fr.	Rh.r
Rhizocarpon viridiatrum (Wulfen) Körb.	Rh.v
Rinodina milvina (Wahlenb.) Th.Fr.	Ri.mi
Schaereria fuscocinerea (Nyl.) Clauzade & Cl.Roux	Sc.f
Staurothele areolata (Ach.) Lettau	St.a
sterile white thallus	St.w
sterile white-greenish	St.wg
Umbilicaria cylindrica (L.) Duby	Um.c
Umbilicaria deusta (L.) Baumg.	Um.d
Verrucaria cfr. *dolosa* Hepp.	Ve.d
Verrucaria nigrescens Pers.	Ve.n
Xanthoparmelia gr. *conspersa* (Ach.) Hale	Xa.c
Xanthoparmelia gr. *pulla* (Ach.) O.Blanco, A.Crespo, Elix, D.Hawksw. & Lumbsch	Xa.p
Xanthoparmelia gr. *stenophylla* (Ach.) Ahti & D.Hawksw.	Xa.s
Xanthoparmelia verruculifera (Nyl.) Essl. O.Blanco, A.Crespo, Elix, D.Hawksw. & Lumbsch	Xa.v
Xanthoria elegans (Link) Th.Fr.	Xa.e

Supplementary Material 4: XRF analyses of metal contents in lichen thalli and comparison between different species found on the same lithotype

Table S4. XRF analyses of metal contents (average % weight ± standard error) in thalli of *Aspicilia caesiocinerea* (A. cae) and *A. cinerea* (A. cin), *Candelariella vitellina* (C. vit), *Lecidella* cfr. *carpathica* (L. car) *Rhizocarpon geographicum* (R. geo), *R. reductum* (R. red), and *R. polycarpum* (R. pol) based on lithology (Dun, dunite; Lhe, lherzolite-harzburgite; Ser_A, serpentinite of Area A; Ser_B, serpentinite of Area B; MMg, Mg-metagabbros)

According to Tukey's test, metal contents measured for the different species which do not share at least one letter are statistically different.

Lithotypes	Mg	Al	Si	Ca	Cr	Fe	Ni	Mg/Ca	Mg/Fe
Dun - A. cae	17.1 (±3)	5.3 (±0.8)	31 (±4.5)	1.9 (±0.2)	0.3 (±0)	42.5 (±0.2)	1.3 (±6.4)	10.3 (±0.4) ab	0.5 (±3.2)
Dun - C. vit	17.8 (±2)	8.8 (±0.8)	38.3 (±2.5)	2.6 (±0.2)	0.3 (±0.1)	30.9 (±0.2)	0.7 (±2.5)	7.3 (±0.3) b	0.6 (±1.1)
Dun - L. car	25.9 (±1.4)	4.6 (±0.6)	32.1 (±2.2)	1.7 (±0.1)	0.2 (±0)	33.9 (±0.1)	1.1 (±2.3)	16 (±0.2) a	0.8 (±1.3)
Dun - R. geo	16.6 (±4.1)	6.2 (±1.3)	36.7 (±4.7)	7.9 (±4.5)	3.2 (±2.7)	29 (±0)	0.4 (±2.4)	5.2 (±0.2) b	0.6 (±2.5)
Dun - R. red	16.9 (±0.9)	8.3 (±0.1)	40.7 (±1.8)	2.1 (±0.2)	0.2 (±0)	31.6 (±0)	0.2 (±2.6)	8.1 (±0.2) ab	0.6 (±0.4)
Lhe - A. cin	10.9 (±2.3)	9.2 (±0.8) bc	45.2 (±3.2) ab	4.1 (±1.2)	1.8 (±1.4)	28.3 (±0.1)	0.2 (±3.3)	5.1 (±0.2)	0.5 (±2.4)
Lhe - C. vit	9.5 (±2)	13.4 (±1.4) a	48.8 (±1.2) b	4.5 (±1)	0.5 (±0.1)	23.1 (±0)	0.3 (±1.7)	3.5 (±0.1)	0.4 (±1)
Lhe - L. car	7.2 (±1.2)	10.9 (±0.3) ab	46.3 (±2.2) ab	5.9 (±1.5)	0.5 (±0.1)	29.2 (±0)	0 (±2.8)	1.6 (±0)	0.3 (±0.4)
Lhe - R. geo	12 (±1.8)	6.7 (±0.7) c	36.9 (±3.2) ab	8.2 (±2.5)	1.1 (±0.2)	34.1 (±0.2)	0.3 (±4.9)	2 (±0.1)	0.5 (±0.3)
Lhe - R. red	13.1 (±2.3)	10.2 (±0.9) abc	50.4 (±3.9) b	4 (±0.7)	0.5 (±0.2)	21.1 (±0.2)	0.3 (±3.5)	4.3 (±0.1)	4 (±1.1)
SerA - A. cin	24.5 (±3.4)	4.9 (±0.7)	36.1 (±1.8)	3.6 (±1.1)	0.8 (±0.2)	29.1 (±0.2)	0.3 (±3.1)	12 (±0.1)	1 (±3.6) ab
SerA - C. vit	15.3 (±1.9)	10.1 (±0.9)	41.2 (±3.6)	4.8 (±0.5)	0.7 (±0.2)	26.6 (±0.2)	0.7 (±3.3)	3.6 (±0.1)	0.6 (±0.7) b
SerA - L. car	14.2 (±3)	9.6 (±1)	39.1 (±5.4)	6.6 (±2.3)	0.2 (±0.1)	29.9 (±0.1)	0.2 (±6.2)	4.1 (±0.1)	0.7 (±1.5) b
SerA - R. geo	28.2 (±5.5)	4.7 (±1)	41.7 (±2)	4.4 (±1.8)	0.5 (±0.2)	19.9 (±0.1)	0.3 (±5.3)	25.9 (±0.1)	2.4 (±12.4) a
SerA - R. red	24.2 (±4.1)	5.4 (±0.9)	38.4 (±2.8)	3.5 (±1)	0.6 (±0.2)	26.8 (±0.1)	0.5 (±3.5)	13 (±0.2)	1 (±5.4) ab
SerB - A. cae	36.1 (±2.4) a	3.5 (±0.7) a	42 (±1.5) ab	5.2 (±2.5)	1.4 (±0.2) a	11.8 (±0) a	0.1 (±1) b	20.2 (±0)	3.2 (±9) a
SerB - C. vit	15.3 (±4) b	11.9 (±1.6) bc	47.7 (±2.3) b	2.5 (±0.6)	0.6 (±0.1) c	21.8 (±0) ab	0.1 (±3.4) b	8.6 (±0.1)	0.8 (±3.9) b
SerB - L. car	23.2 (±6.1) ab	8.2 (±1.9) ab	48.6 (±2.7) b	2 (±0.5)	0.9 (±0.2) abc	17.1 (±0) ab	0 (±1.7) b	21.9 (±0)	1.5 (±10.2) b
SerB - R. geo	18.7 (±4.3) ab	8 (±1.4) ab	36.5 (±1.9) ab	7.6 (±2.8)	1.4 (±0.2) abc	26.8 (±0) b	1 (±3.7) a	4.4 (±0.3)	0.8 (±2) b
SerB - R. pol	17.9 (±7) ab	9.8 (±2.6) ab	47.4 (±3.4) b	8 (±6.1)	0.6 (±0.3) bc	16.3 (±0) ab	0.1 (±2.3) b	13 (±0)	1.1 (±9) b
MMg - A. cin	2.8 (±1.2)	13.1 (±0.3)	61.3 (±2.1)	6.8 (±0.6) ab	0.1 (±0.1)	15.7 (±0.1)	0 (±1.5)	0.4 (±0) b	0.2 (±0.2)
MMg - C. vit	4.3 (±0.4)	14.3 (±0.4)	51.3 (±2.8)	2.5 (±0.4) a	0.3 (±0)	27.1 (±0.1)	0 (±3.8)	1.9 (±0) a	0.2 (±0.2)
MMg - R. geo	2.6 (±1.8)	13.9 (±1.9)	49.5 (±7.3)	9.3 (±2.5) b	0.2 (±0.2)	24.3 (±0)	0 (±5.1)	0.3 (±0) c	0.1 (±0.2)

Supplementary Material 5: Secondary metabolites detected in the developed chromatograms

Table S5. Lichen secondary metabolites detected in the developed chromatograms

Metabolic profiles were examined for seven different species: *Aspicilia caesiocinerea*, A.cae, and *A. cinerea*, A.cin; *Candelariella vitellina*, C. vit; *Lecidella* cfr. *carpathica*, L. car; *Rhizocarpon geographicum,* R. geo; *R. reductum*, R. red, and *R. polycarpum*, R. pol. The occurrence of a metabolite with a certain retention factor (R_f) and a certain colour under short wave UV (Col: orange, or; yellow/yellowish, ye; blue/bluish, bl; red, r; violet, vi; pink, pi; dull, d-; light, l-; pale, p) is marked with black (identified metabolites; Orange *et al.* 2010), dark grey (hypothesized metabolites), and light grey (un-identified metabolites) bars. Metabolites with the same retention factor and colour, but which were detected in different species, are listed separately when their identity is not defined and their analogy is thus uncertain. It is worth noting that more spots than expected, based on accounts in the literature, were observed in the investigated species, as is frequently experienced when performing TLC on lichens.

R_f	Col	Secondary metabolite	A.cae A.cin	C.vit	L.car	R.geo	R.red R.pol
90	ye-or	pulvic acid lactone		■			
88	ye-or	calycin		■			
79	ye	atranorin			■		
68	bl	n.i.		░			
68	br-or	cfr. 2,5,7-trichloro-3-O-methylnorlichexanthone			▓		
65	ye	n.i.		░			
65	r	n.i.	░				
65	or	rhizocarpic acid				■	■
63	br-vi	cfr. chodatin			▓		
63	pi-or	n.i.				░	
60	r	n.i.	░				
58	ye	n.i.		░			
57	or	n.i.	░				
55	ye	n.i.		░			
55	ye	n.i.	░				
49	d-or	cfr. thiophanic acid			▓		
48	or	n.i.		░			
48	ye	n.i.					░
42	l-bl	psoromic acid				■	
40	ye	n.i.	░				
38	p-or	cfr. (iso-)arthotelin			▓		
38	ye	n.i.					░
30	gr	norstictic acid	■				■
28	l-bl-vi	n.i.				░	
28	vi	n.i.			░		
22	bl	n.i.			░		
22	bl	n.i.	░				
20	bl	n.i.		░			
20	ye	n.i.				░	
20	bl	n.i.					░
18	gb	n.i.	░				
18	l-bl	stictic acid					■
15	ye	n.i.				░	
12	ye	n.i.			░		
12	bl-vi	cfr. substictic	▓				
10	ye	n.i.				░	
10	or	n.i.				░	
10	ye	n.i.		░			
10	ye	n.i.					░
10	or	n.i.	░				
8	ye	n.i.	░				
7	ye-or	pulvinic acid		■			
7	vi	n.i.				░	
6	l-bl	n.i.					░
4	or	n.i.	░				
4	bl	n.i.	░				
3	ye-or	connorstictic acid	■				■
1	ye	n.i.				░	

Supplementary Material 6: Detailed comments on PCoA-IIa/e and CCAa/e analyses (see also Fig. 3 and 4 in the main text)

Table S6a. ***Aspicilia caesiocinerea*** **and *A. cinerea* – TLC on *Aspicilia* specimens highlighted a strong difference in the metabolic patterns of populations occurring on Lhe, Ser_A, and MMg, with all thalli producing norstictic acid and related compounds (connorstictic, cfr. substictic) assignable to *A. cinerea*, with respect to those on Dun and Ser_B, never secreting norstictic acid and recognized as *A. Caesiocinerea***

Accordingly, PCoA-IIa (Fig. 3*a*), which extracted 4 components accounting for 81.9% of the total variance, separated along the first axis (45.1% of total variance) the specimens from Lhe, Ser_A, and MMg, being positively correlated with norstictic acid and related compounds (left side of the diagram), from those of the other substrates, which were positively correlated with an undefined substance with R_f=22 (right side of the diagram). The second axis (17.6%) was positively correlated with two undefined substances with R_f=55 and R_f=60, observed in a part of both the subsets of norstictic-containing and norstictic-lacking specimens. CCA-a (Fig. 4*a*) extracted four axes, accounting for 100% of species-environmental relationships, which were all significant (Monte Carlo test, P-value = 0.002). The first axis (53.8%) was positively correlated with Ni (the environmental factor exhibiting the highest conditional effect according to forward selection: F-value 5.22, P-value = 0.002), Fe (F-value 4.74, P-value = 0.002), and Mg (F-value 1.41), and negatively with Si (F-value 4.07, P-value = 0.002), Al, Ca, and Cr (no conditional effect). Norstictic acid, with related compounds, and the undefined substance with R_f=22 showed negative and positive correlations with the first axis (and thus with Ni, Fe, and Mg), respectively.

PCoA-a					
Axes	**1**	**2**	**3**	**4**	**Total variance**
Eigenvalues	0.451	0.176	0.119	0.073	1.000
Cumulative percentage variance of species data	45.1	62.7	74.6	81.9	

CCA-a					
Axes	**1**	**2**	**3**	**4**	**Total inertia**
Eigen values	0.456	0.226	0.113	0.052	2.052
Species-environment correlations	0.900	0.922	0.558	0.446	
Cumulative percentage of variance					
- of species data	22.2	33.3	38.8	41.3	
- of species-environmental relation	53.8	80.5	93.8	100.0	
Monte Carlo Test	**F-ratio**	**P-value**			
Test of significance of first canonical axis	7.149	0.002			
Test of significance of all canonical axes	4.402	0.002			
Marginal and Conditional effects	**λ1**	**λA**	**F-value**	**P-value**	
Ni	0.32	0.32	5.22	0.002	
Fe	0.17	0.26	4.74	0.002	

Si	0.24	0.20	4.07	0.002
Mg	0.20	0.07	1.41	0.186

Table S6b. ***Candelariella vitellina*** **– TLC on *Candelariella vitellina* revealed some differences in the populations from the two investigated areas. Spots at R_f=90, 88, and 7, assigned to pulvinic dilactone, calycin, and pulvinic acid, respectively, were observed in all the specimens**

However, specimens from Area A displayed an orange spot at R_f=48, while thalli from Area B displayed a yellow spot with R_f=10. Accordingly, PCoA-IIb (Fig. 3*b*), which extracted 4 components accounting for 86.1% of the total variance, separated specimens from Area A (right side of the diagram) and Area B (left side of the diagram) along the first axis (40.2% of total variance). In CCA-b (4 extracted axes accounting for 100% of species-environment relationships, with all being significant; Fig. 4*b*), these metabolites scattered separately along the first axis (69%), which showed maximum positive correlation with Ca, exhibiting the highest conditional effect (F-value: 4.10, P-value = 0.002), and maximum negative correlation with Si (F-value: 1.23).

		PCoA-b			
Axes	**1**	**2**	**3**	**4**	**Total variance**
Eigen values	0.402	0.281	0.098	0.079	1.000
Cumulative percentage variance of species data	40.2	68.3	78.1	86.2	
		CCA-b			
Axes	**1**	**2**	**3**	**4**	**Total inertia**
Eigen values	0.161	0.050	0.020	0.003	0.931
Species-environment correlations	0.847	0.521	0.398	0.197	
Cumulative percentage of variance					
- of species data	17.3	22.7	24.8	25.1	
- of species-environmental relation	69.0	90.4	98.8	100.0	
Monte Carlo Test	**F-ratio**	**P-value**			
Test of significance of first canonical axis	5.024	0.002			
Test of significance of all canonical axes	2.011	0.002			
Marginal and Conditional effects	**λ1**	**λA**	**F-value**	**P-value**	
Ca	0.12	0.12	4.10	0.002	
Ni	0.06	0.05	1.53	0.168	
Si	0.06	0.03	1.23	0.308	
Mg	0.04	0.03	1.04	0.414	

Table S6c. *Lecidella carpathica* – All of the specimens of *Lecidella* collected on the four ultramafic substrates displayed a common signature of three metabolites, having R_f=79 (yellowish), 63 (brown violet) and 49 (dull red)

Remarkably, these spots do not show R_f values and spot colours compatible with the metabolites expected in the species of genus *Lecidella* widely reported on siliceous rocks of the Alps, namely *L. carpathica* (atranorin: R_f=79, yellowish; diploicin: R_f=67, colourless; thuringione: R_f=48, but bright orange). On the other hand, these spots are compatible with the metabolites of *L. granulosula* (syn. *L. chodatii*; in Leuckert and Knoph 1992), which has been reported on base-rich siliceous rocks from the central Alps (Nimis and Martellos 2008). However, anatomical features of the apothecia of these specimens were compatible with those described for *L. carpathica* (e.g. red-brown hypothecium) and not with those of *L. granulosula* (e.g. colourless to light brown hypothecium) (Kantvilas and Elix 2013). As specimens from Area B mostly produced an additional metabolite with R_f=38, compatible with (iso-) artothelin, the PCoA analyses (100% of total variance explained by the 4 extracted components), separated them along the first axis (43.4% of total variance), on the right side of the diagram (Fig. 3c). A small group of specimens from Area A also scattered separately from the main set according to their production of an undefined metabolite with R_f=28. In CCA-c (3 extracted axes accounting for 100% of species-environment relationships, with all being significant; Fig. 4*c*), the first axis (85.2%) was positively correlated with Cr, having the highest conditional effect (F-value:6.88, P-value = 0.002), and with the occurrence of the metabolite with R_f=38, separating Ser_B from the other lithologies.

PCoA-c					
Axes	**1**	**2**	**3**	**4**	**Total variance**
Eigen values	0.434	0.286	0.207	0.072	1.000
Cumulative percentage variance of species data	43.4	72.1	92.8	100.0	

CCA-c					
Axes	**1**	**2**	**3**	**4**	**Total inertia**
Eigen values	0.133	0.022	0.001	0.164	0.558
Species-environment correlations	0.825	0.375	0.096	0.000	
Cumulative percentage of variance					
- of species data	23.7	27.7	27.9	57.3	
- of species-environmental relation	85.2	99.3	100.0		
Monte Carlo Test	**F-ratio**	**P-value**			
Test of significance of first canonical axis	6.535	0.002			
Test of significance of all canonical axes	2.703	0.004			
Marginal and Conditional effects	**λ1**	**λA**	**F-value**	**P-value**	
Cr	0.13	0.13	6.88	0.002	
Ca	0.08	0.02	1.38	0.230	
Mg	0.05	0.01	0.08	0.988	

Table S6d. ***Rhizocarpon geographicum*** **– TLC on** ***Rhizocarpon geographicum*** **displayed rhizocarpic acid in all the specimens and psoromic acid in all out of four specimens (three of which on Ser_B). PCoA-IId (Fig. 3*d*), which extracted four components accounting for 79.7% of the total variance, separated along the first axis (33.7% of the total variance) specimens secreting undefined metabolites with R_f=20 and R_f=28, respectively, variously occurring on the different lithologies**

The second axis (20.3%) is positively correlated with undefined metabolites with R_f=1 and R_f=63, mostly, but not exclusively, characterizing the population on MMg. In CCA-d (4 extracted axes accounting for 100% of species-environmental relationships, with all being significant; Fig. 4*d*), these metabolites, with R_f=1 and R_f=63, were positively correlated with the first axis (72.4%), positively correlated with Al (exhibiting the highest conditional effect; F-value: 5.83, P-value = 0.002), Ca, and Si (no conditional effect). These metabolites were negatively correlated with Cr (F-value: 1.68), Ni (F-value: 0.83), and Mg (F-value: 0.26). The metabolites with R_f=28 and R_f=20 showed a positive and negative correlation, respectively, with the second axis (17.8%), positively correlated with Ca and Cr. It is worth noting that the same metabolite patterns also characterized the population of *R. viridiatrum* observed on Lhe and Dun in Area A and on MMg in Area B (data not shown).

PCoA-d					
Axes	**1**	**2**	**3**	**4**	**Total variance**
Eigenvalues	0.337	0.203	0.142	0.115	1.000
Cumulative percentage variance of species data	33.7	54.0	68.2	79.7	
CCA-d					
Axes	**1**	**2**	**3**	**4**	**Total inertia**
Eigenvalues	0.217	0.056	0.025	0.001	1.185
Species-environment correlations	0.892	0.485	0.429	0.100	
Cumulative percentage of variance					
- of species data	18.3	23.0	25.2	25.3	
- of species-environmental relation	72.4	91.2	99.6	100.0	
Monte Carlo Test	**F-ratio**	**P-value**			
Test of significance of first canonical axis	5.606	0.002			
Test of significance of all canonical axes	2.115	0.002			
Marginal and Conditional effects	**λ1**	**λA**	**F-value**	**P-value**	
Al	0.20	0.20	5.83	0.002	
Cr	0.15	0.06	1.68	0.114	
Ni	0.03	0.03	0.83	0.574	
Mg	0.14	0.01	0.26	0.968	

Table S6e. ***Rhizocarpon reductum*** **and** ***R. polycarpum*** **– All of the specimens of** ***Rhizocarpon reductum*** **on the three lithologies found in Area A produced stictic acid**

Norstictic and rhizocarpic acids were present in all specimens from Lhe, but only in a subset of those from Dun and Ser_A. Similarly, on Ser_B, the investigated specimens of *R. polycarpum* contained stictic acid, but only one and two of them, respectively, produced norstictic and rhizocarpic acids. PCoA-IIe (Fig. 3*e*), which extracted four components accounting for 91.2% of the total variance, showed along the first axis (36.8% of total variance) the separation between specimens producing norstictic and/or rhizocarpic acids (on the left side of the diagram) and the others (on the right side). The second axis (27.0%) separated specimens producing only one of the two acids (norstictic acid in the upper side of the diagram, rhizocarpic acid in the lower side). In CCA-e (3 extracted axes accounting for 100% of species-environmental relationships, with all being significant; Cr and Ni omitted because of negligible variance; Fig. 4*e*), the first axis (50.9%) was negatively correlated with Fe (exhibiting the highest conditional effect; F-value: 3.02; P = 0.010), and Mg (F-value: 0.95), while positively correlated with Al (F-value: 2.28), Si, and Ca. Both norstictic and rhizocarpic acids scattered on the right side of the diagram, exhibiting a positive correlation with axis 1.

PCoA-e					
Axes	**1**	**2**	**3**	**4**	**Total variance**
Eigenvalues	0.368	0.270	0.159	0.114	1.000
Cumulative percentage variance of species data	36.8	63.8	79.8	91.2	

CCA-e					
Axes	**1**	**2**	**3**	**4**	**Total inertia**
Eigenvalues	0.143	0.101	0.037	0.305	1.069
Species-environment correlations	0.614	0.672	0.608	0.000	
Cumulative percentage of variance					
- of species data	13.4	22.9	26.3	54.9	
- of species-environmental relation	50.9	86.9	100.0		
Monte Carlo Test	**F-ratio**	**P-value**			
Test of significance of first canonical axis	2.783	0.100			
Test of significance of all canonical axes	2.144	0.02			
Marginal and Conditional effects	**λ1**	**λA**	**F-value**	**P-value**	
Fe	0.14	0.14	3.02	0.010	
Al	0.12	0.10	2.28	0.054	
Mg	0.12	0.04	0.95	0.422	

Supplementary Material 7: Pull up tests – image analysis of detached mineral fragments

Image analysis by WinCAM was used to count the detached mineral fragments per cm^{-2} on the adhesive tape applied to the bare surfaces of the different lithologies to discriminate different patterns of disaggregation. The detachment of a few millimetre-scale mineral fragments commonly characterized Ser_A, Ser_B and MMg, while a yellowish-rusty micrometre-scale mineral powder, likely related to olivine weathering, was uniformly detached from the Dun surface. Similar gravimetric results obtained for Dun and MMg are thus considered to be related to very different disaggregation patterns (see Fig. S7). It is worth noting that, in the case of Dun and Lhe, even a higher number of particles was detached with respect to the reported values, but image analysis failed to count the finest fraction, which was instead observed by microscopy. Moreover, in the case of Lhe, the lumpy appearance related to clinopyroxene phenocrysts partially affected the application of the adhesive tape, likely determining an underestimation of the detached fragments.

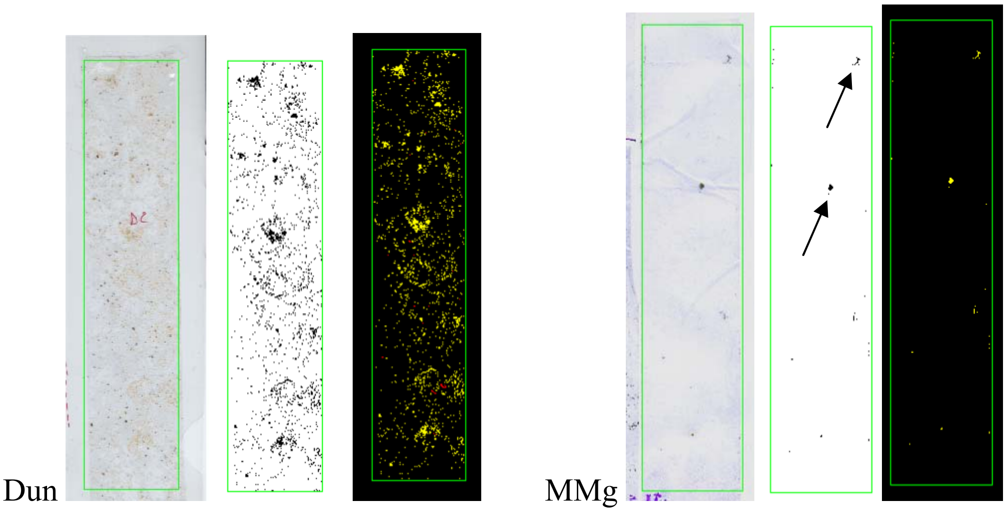

Fig. S7. Detachment of mineral fragments from the bare surface of Dun and MMg, displaying similar results in terms of gravimetric analysis, but different disaggregation patterns (arrows indicate millimetre-scale detached fragments).